Brain Stimulation 12 (2019) 161–174

Contents lists available at ScienceDirect

Brain Stimulation

journal homepage: http://www.journals.elsevier.com/brain-stimulation

The neuroprotective effect of deep brain stimulation at nucleus basalis of Meynert in transgenic mice with Alzheimer's disease

Chuyi Huang [a, 1], Heling Chu [b, 1], Yu Ma [c], Zaiying Zhou [d], Chuanfu Dai [e], Xiaowen Huang [f], Liang Fang [g], Qiang Ao [h, *], Dongya Huang [a, **]

[a] Department of Neurology, Shanghai East Hospital, Tongji University School of Medicine, No. 150 Jimo Road, Shanghai 200120, China
[b] Department of Neurology, Huashan Hospital, Fudan University, No.12 Mid. Wulumuqi Road, Shanghai 200040, China
[c] Department of Neurosurgery, Tsinghua University Yuquan Hospital, No. 5 Shijingshan Road, Shijingshan District, Beijing 100049, China
[d] Center for Statistical Science of Tsinghua University, Beijing 100084, China
[e] Department of Otolaryngology, Head and Neck Surgery, Beijing Tsinghua Changgung Hospital, School of Clinical Medicine, Tsinghua University, Beijing 102218, China
[f] Department of Orthopedics, Jiangsu Province Hospital, The First Affiliated Hospital of Nanjing Medical University, Nanjing 210029, China
[g] Department of Mathematical Sciences, Tsinghua University, Beijing 100084, China
[h] Department of Tissue Engineering, China Medical University, No. 77 Puhe Road, Shenyang Liaoning, 110122, China

ARTICLE INFO

Article history:
Received 6 March 2018
Received in revised form
19 August 2018
Accepted 22 August 2018
Available online 27 August 2018

Keywords:
Alzheimer's disease
Deep brain stimulation
Nucleus basalis of Meynert
APP/PS1 transgenic mice
Morris water maze

ABSTRACT

Background: Alzheimer's disease (AD) is the most common type of dementia and mainly treated by drugs, while the therapeutic outcomes are very limited. This study aimed to determine the optimized parameters of deep brain stimulation (DBS) which was applied to the treatment of AD and propose the involved mechanisms.

Methods: Amyloid-β precursor protein/Presenilin1 (APP/PS1) transgenic mice were used and received DBS at nucleus basalis of Meynert (NBM). The optimized parameters of DBS were determined by using different stimulation frequencies, durations and ages of mice under Morris water maze test. The involved mechanisms and the possible signal pathways were also investigated.

Results: The optimized parameters for DBS were high frequency (100 Hz) for 21 days starting from early age (4 months old). Under the above parameters, the soluble Aβ40 and Aβ42 in the hippocampus and cortex were down-regulated significantly. DBS increased survival neurons and reduced apoptotic cells in the hippocampus and cortex. Meanwhile, the apoptosis-related proteins caspase-3, caspase-8 and Bid were down-regulated. Moreover, DBS caused a significant increase of superoxide dismutase, glutathione peroxidase and choline acetyltransferase activity as well as a decrease of methane dicarboxylic aldehyde content and acetylcholine esterase activity. Phosphorylation of Akt (*p*-Akt)/total Akt (t-Akt) was up-regulated while p-extracellular signal-regulated kinase 1/2 (ERK1/2)/t-ERK1/2 was down-regulated. The neuroprotective effect of DBS was attenuated by their inhibitors.

Conclusions: NBM-DBS starting from 4 months of age for 21 days at a high frequency (100 Hz) has therapeutic effects on AD through activating phosphatidylinositol 3′-kinase (PI3K)/Akt pathway and inhibiting ERK1/2 pathway.

1. Introduction

Alzheimer's disease (AD) is the fourth leading cause of death among the elderly, posing a great threat to global public health. At present, medication seems to be the only solution for AD, though drugs only delay the progression of AD rather than radically cure AD.

Deep brain stimulation (DBS) produces mild, continuous electrical pulses to the neural nuclei of the brain. Compared with the

* Corresponding author.
** Corresponding author.
E-mail addresses: aoqiang@tsinghua.edu.cn (Q. Ao), dongyahuang77@hotmail.com (D. Huang).
[1] These authors contributed equally to this work.

https://doi.org/10.1016/j.brs.2018.08.015
1935-861X/

ablative procedure, DBS has the following advantages: (1) Minimally invasive and not destructive for brain tissues [1]; (2) controllable; (3) repeatably switching on and off of the DBS device to conduct evaluation; (4) reversible side effects. DBS has been applied to movement disorders, epilepsy and psychiatric disorders at present. Pre-clinical research indicates that DBS may alter development of AD by interfering with the pathophysiological changes of the brain. Therefore, DBS may be also applied to cognitive impairment [2,3].

To date, several studies with small sample size have focused on the effect of DBS on AD patients. The choice of target regions is directly associated with the outcomes. According to the studies, fornix and nucleus basalis of Meynert (NBM) are two main DBS targets which can help trigger the cognitive loop and thus improve the learning and memory capacities [4]. It was demonstrated that DBS at fornix reduced hippocampus atrophy and increased brain glucose metabolism [5,6]. However, a recent phase II study indicated fornix-DBS failed to improve cognitive functions of all participants [7]. Another crucial target is NBM which represents an important cholinergic pathway in the cognition and memory functional network. The projecting fibers originating from NBM are mainly found in hippocampus, amygdaloid nuclei, hypothalamus, thalamus and prefrontal cortex, which are structures associated with memory and cognition [8]. Acetylcholine (ACh) is the key neurotransmitter involved in memory function and also related to the development of AD. DBS at NBM can improve cognitive function and promote synthesis and release of ACh [9,10]. Moreover, a pilot study of six patients revealed DBS at NBM ameliorated AD-associated symptoms, with increased cerebral glucose consumption [11]. Therefore, NBM is considered as a potential target for DBS in cognitive dysfunction patients, including those with AD. However, little is known about the effect of long-term DBS at NBM on cognitive improvement of AD patients. Similarly, no animal experiments have been performed to investigate the involved mechanisms.

In this study, the amyloid-β precursor protein/presenilin1 (APP/PS1) mouse as an AD model was used for long-term DBS, so as to determine the optimized stimulation frequency, starting time and duration of treatment, and to explore the working mechanisms.

2. Methods

2.1. Laboratory animals

Healthy SPF C57/BL6-Tg transgenic mice (HuAPP695swe, PSEN1-dE9) aged 10 weeks were purchased from Model Animal Research Center of Nanjing University (license: SCXK [Jiangsu] 2010–0111). Wild type (WT) C57BL/6 mice were used as controls. All mice were males, with an average body weight of 28 ± 2.4 g. They were reared under barrier conditions for rodents (temperature 24 ± 1.5 °C, 50% humidity) at Laboratory Animal Center of Tsinghua University, which was accredited by Association for Assessment and Accreditation of Laboratory Animal Care. The mice were allowed free access to clean food and water, and acclimatized in a 12 h/12 h light/dark cycle for 7 days. The protocol was approved by the Institutional Animal Care and Use Committee of Tsinghua University.

2.2. Microelectrode implantation

Except the control group, all WT and APP/PS1 transgenic mice were implanted by stainless steel microelectrodes (MS303-3-B-SPC, Plastics One, Roanoke, USA) (bipolar, twisted; bare electrode diameter, 0.125 mm; insulated electrode diameter, 0.150 mm; impedance control range, 15–45 kΩ) at NBM. The electrical stimulator was 30 mm in length with a diameter of 8 mm and provided biphasic stimulus pulse wave. The steps for microelectrode implantation were as follows: (1) Anesthesia: The mice were fasted from food and water for 5 and 3 h, respectively, before the experiment. Anesthesia was performed by isoflurane via a mask (3% for induction, 1–1.5% for maintenance in 70% nitrous oxide and 30% oxygen). (2) Fixation of ear rods: After anesthesia, two stainless steel ear rods of the stereotactic instrument (Narishige Company Limited) were inserted into bilateral ears of mice and fixed well. To ensure that the ear rods were accurately positioned, the mice with the inserted ear rods were placed on the stereotactic instrument, and the ear rods were adjusted so that the readings were consistent from the scale. Then the incisors of the mice were immobilized in the incisor groove in front of the stereotactic instrument. (3) Removal of the scalp to expose the skull: The hairs near the surgical field were removed, and the scalp behind the eyes and in front of the ears was disinfected with iodophor. Part of the scalp in the surgical area was removed by cutting. Blunt dissection was performed and the scalp fascia was torn apart to expose the skull. The soft tissues on the skull surface were eroded with 3% hydrogen peroxide using a cotton ball until the surface of the skull became white and the anterior fontanelle and posterior fontanelle were clearly seen. (4) Microelectrode implantation: The microelectrode was mounted and fixed to the stereotactic instrument, and collimation was done with a hanging string. The height of the incisor was adjusted so that the anterior and posterior fontanelles were located on the same level. A hole of 2 mm in diameter was drilled gently on the skull using a dental bur and the damage to the dura mater was avoided. Stereotactic surgery was performed to implant the microelectrode to the left NBM under the following parameters: NBM: Bregma, −0.7 mm; Lateral, 1.75 mm; Ventral, 4.0 mm [12]. (5) Microelectrode fixation: After the microelectrode was implanted to the left NBM, one drop of glue was added to seal the cranial foramina. Then the microelectrode was fixed to the skull using a large amount of acrylic denture base materials. After making an incision between the shoulder blades, the stimulator was implanted subcutaneously on the back of the mice. Carprofen (5 mg/kg) was subcutaneously administered at 12 and 24 h after surgery to reduce pain and then scratch the electrical stimulator. After surgery, the mice were returned to the cage and rested for 7 days. Mice were kept separately to avoid microelectrodes dropping off induced by other mice. The integrity of the electrical stimulators was checked daily. Microelectrodes dropping off occurred in two mice, which were timely handled (Fig. 1A–D).

2.3. Experimental procedures and groups

Three parts of experiments were included in the current work. Six mice were included for each parameter of each group. A total of 168 APP/PS1 mice and 24 WT mice were enrolled in the study (Fig. 1E).

Part 1: Optimized DBS parameters selection for AD treatment. APP/PS1 mice were randomly divided into three groups: Group 1 (Control), Group 2 (Sham stimulation), and Group 3 (DBS). 6-month-old mice were first selected and given different frequencies (10 Hz, 50 Hz, 100 Hz and 130 Hz) of freely-moving stimulation with a pulse width of 90 μs and intensity of 1 A, for 60 min per day (13:01–14:00 pm). Morris water maze (MWM) test was done after 30-day stimulation. Then different starting time of DBS (4, 6, 9 and 12 months of age) was selected, and the optimized frequency was used for 30-day stimulation. In our preliminary experiment, different starting time of sham stimulation displayed similar results of MWM test due to the absence of stimulation. To make the figure more succinct, the data from the starting time of 12 months for the control and sham stimulation groups were used. MWM test was conducted at the end of 13 months of age for each

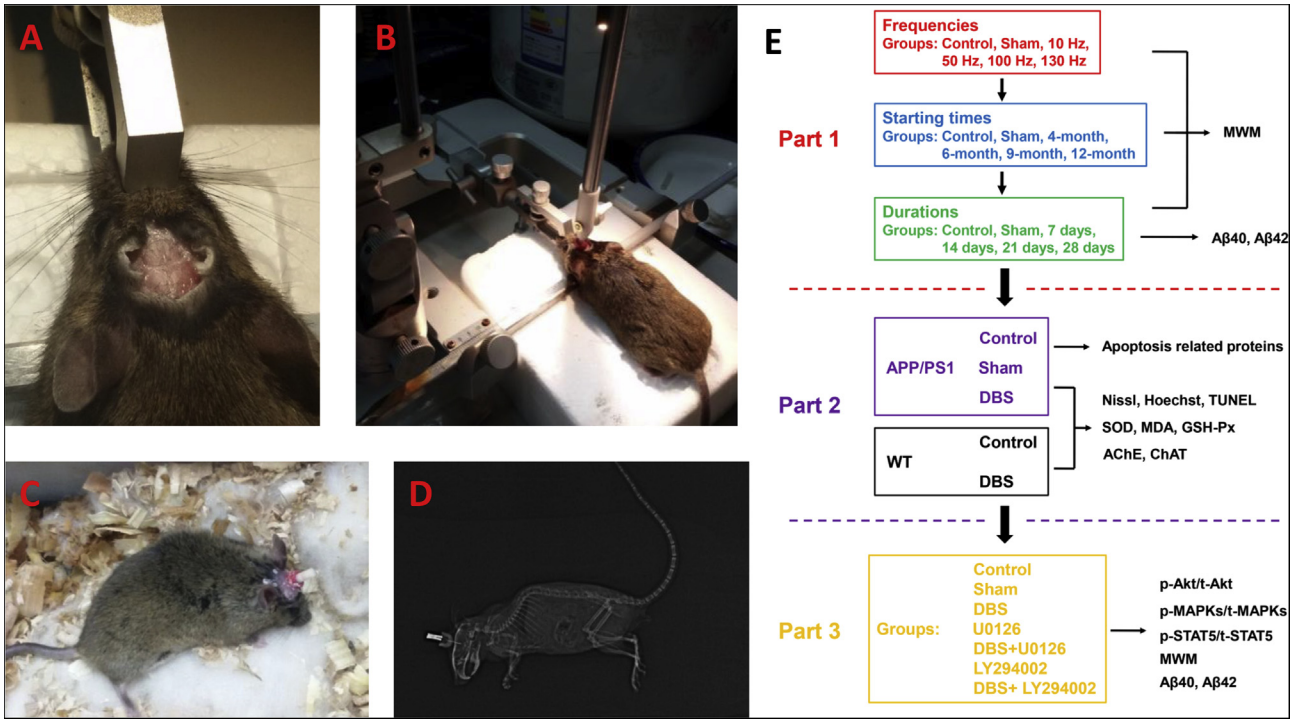

Fig. 1. The procedures of microelectrode implantation and a schematic of experimental groups and procedures. (A) Exposure of the skull. (B) Microelectrode implantation. (C) Microelectrode fixation. (D) X-ray showed the microelectrode was implanted at the proper location and well fixed. (E) A schematic of experimental groups and procedures.

group of mice. Subsequently, optimized durations were explored from four different durations (7 days, 14 days, 21 days and 28 days) with the selected optimized frequency and starting time. MWM and amyloid-β40 (Aβ40) and Aβ42 levels were detected at the end of 30 days after DBS.

Part 2: Investigation on the mechanisms of the therapeutic effects of DBS on AD. WT mice and APP/PS1 mice were randomly divided into five groups: Group 1 (WT control), Group 2 (WT DBS), Group 3 (APP/PS1 control), Group 4 (APP/PS1 sham stimulation), and Group 5 (APP/PS1 DBS). The optimized DBS parameters were employed, and the role of DBS in neuronal survival, apoptosis, oxidative stress and ACh metabolism was investigated.

Part 3: Study on the possible signal transduction pathways. APP/PS1 mice were randomly divided into five groups: Group 1 (Control), Group 2 (Sham stimulation), Group 3 (DBS), Group 4 [DBS plus U0126, 150 μg/kg, Invivogen, San Diego, USA, an extracellular signal-regulated kinase 1/2 (ERK1/2) inhibitor], and Group 5 [DBS plus LY294002, 150 μmol/L, Invivogen, a phosphatidylinositol 3′-kinase (PI3K) inhibitor]. Ratios of phosphorylation/total Akt, ERK1/2, C-Jun amino-terminal kinase (JNK), p38-mitogen-activated protein kinase (MAPK) and signal transducer and activator of transcription 5 (STAT5) were detected. Meanwhile, the effects of inhibitors were also investigated. U0126 and LY294002 were injected intracerebroventricularly (0.9 mm lateral to the midline, and 0.1 mm posterior to the coronal suture, with a depth of 3.1 mm from the surface of the brain) at 0 day, 7 days and 14 days after DBS. The doses of drugs were determined according to our preliminary experiment and previous reports [13,14].

2.4. MWM test

Spatial memory and learning were evaluated using MWM test as previously described [15]. The apparatus consisted of black circular pool which was 116 cm in diameter and 60 cm in height, and was divided into four quadrants and filled with water. In the room, many clues external to the maze (e.g., pictures on the walls, lamps, and a camera on the ceiling) were visible from the pool and presumably used by the mice for spatial orientation. The position of the cues remained unchanged throughout the experiment. An escape platform (10 cm in diameter) was submerged 1 cm below the water surface in the third quadrant (the target quadrant). The mice were placed in the water randomly from four quadrants and trained for six consecutive days to find the submerged platform. The maximum time for which the mice were allowed to swim was 120 s. If an animal failed to find the escape platform within 120 s, the experimenter would guide it. Latency to reach the platform and swimming speed were automatically calculated by the video tracking system (Dig-Behav, Jiliang Co. Ltd., Shanghai, China). In the space exploration task, the platform was removed. The mice were placed in the water randomly from four quadrants and allowed to search for the platform during 60 s. The same video tracking system was used to record the number of passes and time of occupancy in the target quadrant and platform area. The observers were blinded to the groups.

2.5. Western blot

Brain was rapidly removed from the skull and tissues of hippocampus were separated (DBS hemisphere), which were performed less than 2 min after the decapitation. Tissues were homogenized in RIPA lysis buffer (Beyotime, Suzhou, China) and 1 mmol/L phenylmethanesulfonyl fluoride (PMSF). After centrifuged at 12000 rpm for 15 min, the supernatant was used for analysis. Proteins (50 μg) were loaded onto 4% stacking/12% separating SDS-polyacrylamide gels for electrophoresis, and then transferred onto nitrocellulose transfer membranes. After blocked, membranes were incubated overnight at 4 °C with anti-caspase-3 (1:1000, Millipore, Billerica, USA, Cat No.: AB1899), anti-caspase-8 (1:1000, Millipore, Cat No.: AB1879), anti-Bid (1:1000, Millipore, Cat No.: AB1730), anti-caspase-9 (1:1000, Millipore, Cat No.:

AB3629), anti-Bax (1:1000, Millipore, Cat No.: AB2915), anti-Bcl-2 (1:1000, Millipore, Cat No.: AB1722), anti-*p*-Akt (1:1000, CST, Boston, USA, Cat No.: 4060), anti-*p*-ERK1/2 (1:1000, CST, Cat No.: 4370), anti-*p*-JNK (1:1000, CST, Cat No.: 4668), anti-p-p38 (1:1000, CST, Cat No.: 4511) and anti-p-STAT5 (1:1000, CST, Cat No.: 4322) rabbit polyclonal antibodies as well as anti-total Akt (t-Akt) (1:1000, CST, Cat No.: 2920), anti-t-ERK1/2 (1:1000, CST, Cat No.: 4696), anti-t-JNK (1:1000, CST, Cat No.: 9252), anti-t-p38 (1:1000, CST, Cat No.: 9217), and anti-t-STAT5 (1:1000, CST, Cat No.: 9356) mouse polyclonal antibodies. Membranes were then incubated for 1 h at room temperature with horseradish peroxidase (HRP) labeled goat anti-rabbit secondary antibody (1:4000, Vector, Burlingame, USA, Cat No.: PI-1000) or horse anti-mouse secondary antibody (1:4000, Vector, Cat No.: PI-2000). The membranes were placed into ECL solution for 5 min, and then exposed. The intensity of blots was quantified using the Leica Image Processing and Analysis System. β-Actin was used as an internal control [16]. After the first experiment, the blots were washed to remove the chemiluminescent substrate and then placed in stripping buffer (Thermo Fisher Scientific, Waltham, USA), followed by incubation for 5–15 min at room temperature. After washed and blocked, the membranes were used for a second immunoprobing experiment.

2.6. Terminal deoxynucleotidyl transferase-mediated dUTP nick end labeling (TUNEL) staining

Mice were anesthetized and perfused with normal saline solution and 4% ice-cold paraformaldehyde through the left cardiac ventricle. Brain tissues from hippocampus of DBS hemisphere were removed and gradient dehydrated. Serial coronal sections (10 μm) were then cut on a freezing microtome (CM, 1900, Leica, Wetzlar, Germany). After washed, the sections were stained for TUNEL using in Situ Cell Death Detection Kit (Roche, Mannheim, Germany) following the manufacturer manual.

2.7. Nissl staining

Brain tissues from hippocampus and cortex of DBS hemisphere were obtained and processed by the method in “TUNEL” part. Sections were stained with toluidine blue (Sigma-Aldrich) for 20 min. After washed by distilled water, sections were separated color with 95% ethanol for 30 s [17].

2.8. Hoechst staining

Brain tissues from hippocampus and cortex of DBS hemisphere were obtained and processed by the method in “TUNEL” part. For Hoechst staining, sections were stained with Hoechst 33258 (Beyotime) for 10 min, rinsed and cleared in ethanol and xylenes, and covered with a cover slip under Permount.

2.9. Cell counting

For cell counting, coronal sections of 10 μm were cut from the optic nerve to mamillary body. Every other section was chosen after hippocampus CA1 region or cortex was first spotted and six sections were selected altogether. Then six nonoverlapping fields per section in the CA1 region or cortex under high power lens (× 400) were randomly chosen. The average was regarded as the cell number of the Nissl or TUNEL or Hoechst staining.

2.10. ELISA for Aβ40 and Aβ42 protein expression

Aβ40 and Aβ42 protein levels were measured using mouse Aβ40 and Aβ42 ELISA kit (R&D Systems Inc., Minneapolis, USA). Sample homogenates preparation and assays were performed according to the manufacturer instructions. The protein levels of Aβ40 and Aβ42 in brain tissues were normalized and expressed as ng per g of total protein.

2.11. Biochemical assay

Brain tissues from hippocampus and cortex were separated by the method in “Western blotting” part. In order to evaluate the oxidative stress status, assay kits were used to measure the activity of superoxide dismutase (SOD), glutathione peroxidase (GSH-Px) and levels of methane dicarboxylic aldehyde (MDA) (Jiancheng Bioengineering Institute, Nanjing, China). Meanwhile, the activity of acetylcholine esterase (AChE) and choline acetyltransferase (ChAT) was also detected by corresponding assay kits (R&D Systems Inc.). Sample homogenates preparation and assays were performed as the manufacturer's instructions.

2.12. Statistical analysis

All data were presented as mean ± SEM and analyzed with SPSS22.0. After tests for normality and homogeneity of variance, differences among multiple groups were compared by using one-way analysis of variance (ANOVA). When the ANOVA identified significant differences, Tukey's honestly significant difference test was used for intergroup comparisons. Differences were considered significant at $p < 0.05$. All analyses were conducted by an observer blinded to the groups.

3. Results

3.1. The effects of different stimulation frequencies in MWM test

DBS was given to APP/PS1 mice at four frequencies (10 Hz, 50 Hz, 100 Hz and 130 Hz). As indicated by place navigation in MWM test, escape latency for locating the platform decreased obviously in each group with a higher number of training trials. DBS at 10 Hz had no effect on escape latency for locating the platform, while DBS at the other three frequencies significantly reduced the latency from the second day of training ($p < 0.05$). DBS at 100 Hz greatly reduced the escape latency at any other time points as compared with other frequencies ($p < 0.05$). However, the number of training trials and stimulation frequencies had no impact on the swimming speed of mice. In the space exploration task, DBS at 10 Hz had no effect. However, DBS at 50 Hz, 100 Hz and 130 Hz all significantly increased the number of passes and time of occupancy in the target quadrant and platform area ($p < 0.05$). Furthermore, the maximum number and time were observed at 100 Hz as compared with other frequencies ($p < 0.05$) (Fig. 2).

3.2. The effects of different stimulation starting time in MWM test

DBS was given to APP/PS1 mice aged 4, 6, 9 and 12 months and MWM test was conducted at the end of 13 months. The results showed that early stimulation (from 4 months of age) could greatly reduce the escape latency as compared with other starting time ($p < 0.05$). DBS at 6 months of age also reduced the escape latency ($p<0.05$). However, DBS at 9 and 12 months of age had bare impact on the latency. But whatever the starting time, the swimming speed of mice was not affected. In the exploration task, DBS at 4 and 6 months of age greatly increased the number of passes and time of occupancy in the target quadrant and platform area ($p < 0.05$). In addition, early stimulation at 4 months of age elicited the optimized effect as compared with any other starting time ($p < 0.05$).

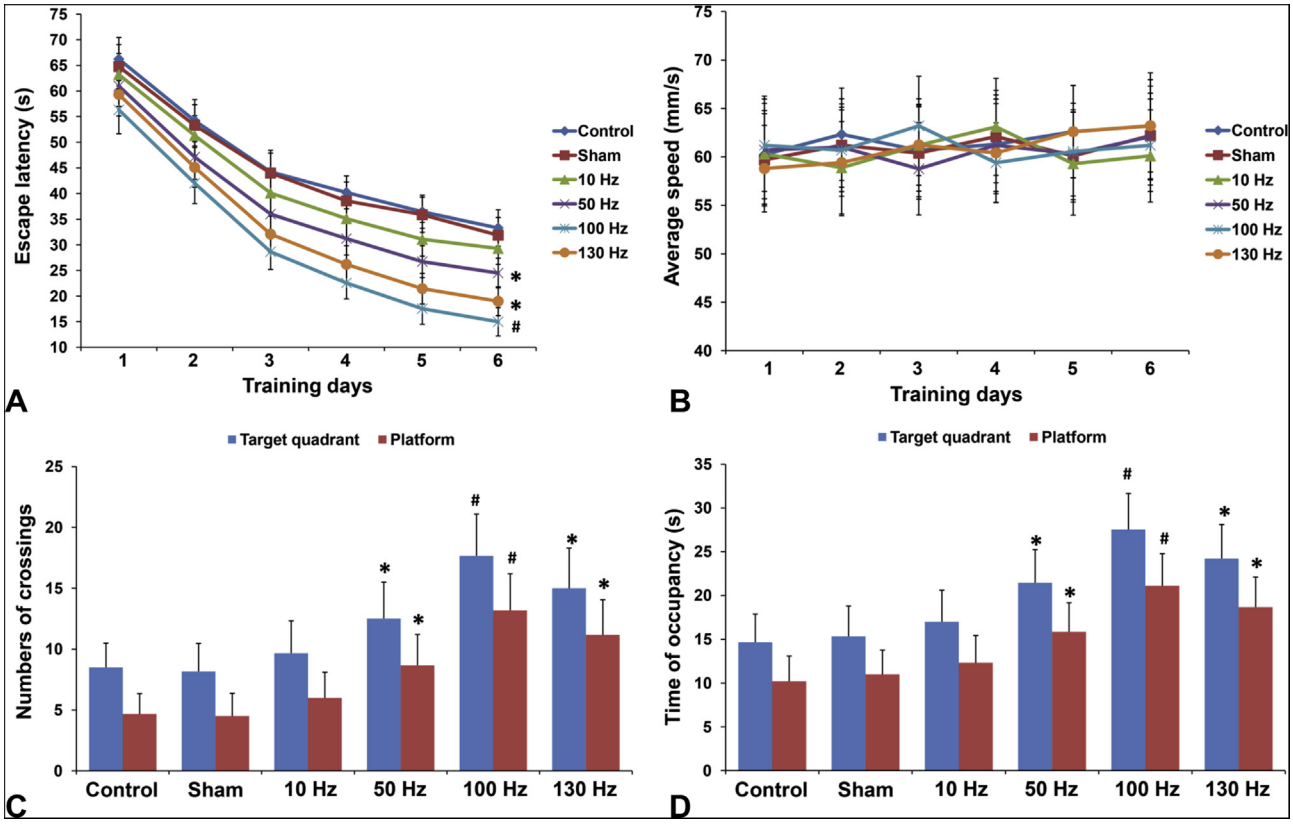

Fig. 2. The effects of different stimulation frequencies in MWM test of APP/PS1 mice. (A) DBS at 50 Hz, 100 Hz and 130 Hz reduced the escape latency, with the greatest reduction at 100 Hz * $p < 0.05$, vs. sham stimulation group from the second training day; #$p < 0.05$, vs. other groups from the second training day. (B) Stimulation frequencies had no impact on the swimming speed. (C, D) DBS at 50 Hz, 100 Hz and 130 Hz all increased the number of passes over the target quadrant and the platform area (C) as well as the time of occupancy in the target quadrant and platform area (D). DBS at 100 Hz group had the maximum number and time. *$p < 0.05$, vs. sham stimulation group; #$p < 0.05$, vs. other groups.

However, stimulation at 9 and 12 months of age had bare impact (Fig. 3).

3.3. The effects of different stimulation durations in MWM test

DBS was given to APP/PS1 mice at four different durations (7 days, 14 days, 21 days and 28 days). Place navigation in MWM test showed that stimulation for 7 days had bare impact on escape latency, while stimulation for 14 days, 21 days and 28 days greatly reduced the escape latency from the second day of training ($p < 0.05$). Stimulation for 21 days significantly reduced the escape latency at all time points as compared with other durations ($p < 0.05$). However, training durations had no impact on the swimming speed of mice. In the exploration task, stimulation for 7 days had bare impact. Stimulation for 14 days, 21 days and 28 days all increased the number of passes and time of occupancy in the target quadrant and platform area significantly ($p < 0.05$). Stimulation for 21 days further increased the number of passes and time of occupancy in the target quadrant and platform area as compared with other durations ($p < 0.05$) (Fig. 4A–D).

3.4. The effects of different stimulation durations on Aβ40 and Aβ42 levels

As indicated by ELISA, DBS for 7 days had no impact on Aβ40 and Aβ42 levels in APP/PS1 mice. DBS for 14 days, 21 days and 28 days could all reduce the soluble Aβ40 and Aβ42 levels in the hippocampus and cortex significantly ($p < 0.05$). DBS for 21 days further reduced Aβ40 and Aβ42 levels as compared with other durations ($p < 0.05$) (Fig. 4E–H). As examined in this section, it was concluded that the optimized parameters for DBS were high frequency (100 Hz) for 21 days starting from early age (4 months of age).

3.5. The effects of DBS on Nissl, Hoechst and TUNEL staining of the hippocampus and cortex

The optimized DBS parameters were used in the following experiments. Nissl staining was employed to evaluate neuronal death resulting from AD, and the positive cells were survival neurons. Hoechst staining and TUNEL staining were employed to detect apoptotic cells. The changing trend of the three kinds of staining cells was shown in microscopic images. Quantitative analysis was made. DBS showed no effect in WT mice. However, DBS increased the number of Nissl positive neurons while decreased Hoechst and TUNEL positive cells in the hippocampus CA1 region and cortex of APP/PS1 mice ($p < 0.05$) (Fig. 5A–C, Fig. 6, Fig. 8A–C).

3.6. The effect of DBS on apoptosis related proteins

Several key apoptosis related proteins were determined by Western blot with semi-quantitative analysis. The results showed that DBS caused a significant down-regulation of caspase-3, caspase-8 and Bid proteins in APP/PS1 mice ($p < 0.05$), while it had no effect on caspase-9, Bax and Bcl-2 expression (Fig. 7).

3.7. The effect of DBS on oxidative stress in each group of mice

Several important oxidative stress-related factors were determined. DBS showed no effect in WT mice. However, it was revealed that DBS greatly enhanced the activity of SOD and GSH-Px in APP/

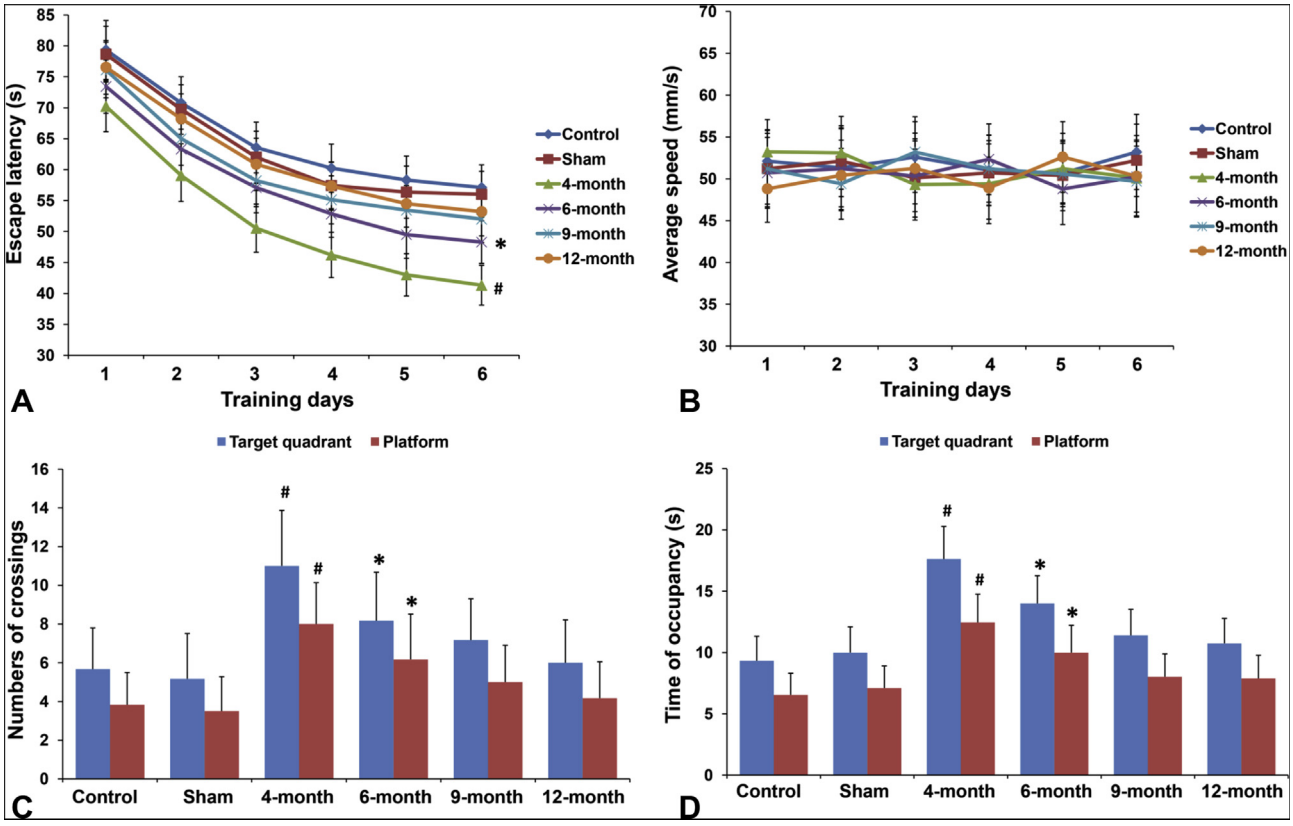

Fig. 3. The effects of different starting time in MWM test of APP/PS1 mice. (A) DBS of the mice at the age of 4 and 6 months reduced the escape latency and the former displayed the greatest reduction as compared with other starting time. $^{*}p < 0.05$, vs. sham stimulation group; $\#p < 0.05$, vs. other groups. (B) The swimming speed of mice was not affected by the starting time. (C, D) DBS of the mice at the age of 4 and 6 months increased the number of passes over the target quadrant and platform area (C) as well as the time of occupancy in the target quadrant and platform area (D). Early stimulation at the age of 4 months elicited the optimized effect. $^{*}p < 0.05$, vs. sham stimulation group; $\#p < 0.05$, vs. other groups.

PS1 mice ($p < 0.05$), while the level of MDA was reduced ($p < 0.05$) (Fig. 8D–F).

3.8. The effect of DBS on the cholinergic system in each group of mice

ChAT and AChE of the cholinergic system were determined. It was demonstrated that DBS greatly increased the ChAT activity in APP/PS1 mice ($p < 0.05$), while reduced AChE activity both in the hippocampus and cortex ($p < 0.05$). However, no such effects were found in WT mice (Fig. 5D and E, Fig. 8G and H).

3.9. The effect of DBS on signaling pathway proteins in APP/PS1 mice

Ratios of phosphorylation/total of Akt, MAPKs and STAT5 were determined by Western blot with semi-quantitative analysis. The data showed that DBS resulted in a significant up-regulation of *p*-Akt/t-Akt and a down-regulation of *p*-ERK1/2/t-ERK1/2 in APP/PS1 mice ($p < 0.05$), while it had no impact on *p*-JNK/t-JNK, p-p38/t-p38 or p-STAT5/t-STAT5 expression (Fig. 9).

3.10. The effect of U0126 on DBS treatment

As indicated by place navigation in MWM test, U0126 reduced the escape latency of APP/PS1 mice ($p < 0.05$). After DBS, U0126 partially counteracted the improvement effect of DBS as represented by the escape latency ($p < 0.05$). However, the latency was still shorter than that after the use of U0126 but no DBS ($p < 0.05$). U0126 had no obvious impact on the swimming speed of mice. In the exploration task, the use of U0126 increased the number of passes and time of occupancy in the target quadrant and platform area ($p < 0.05$). After DBS, U0126 attenuated but did not counteract the improvement effect of DBS as represented by the number of passes and time of occupancy in the target quadrant and platform area ($p < 0.05$). Similarly, ELISA showed that U0126 reduced soluble Aβ40 and Aβ42 levels in APP/PS1 mice ($p < 0.05$). After DBS, U0126 partially counteracted the improvement effect of DBS as represented by Aβ40 and Aβ42 levels ($p < 0.05$). However, Aβ40 and Aβ42 levels were still lower than those with the use of U0126 but no DBS ($p < 0.05$) (Fig. 10).

3.11. The effect of LY294002 on DBS treatment

According to place navigation in MWM test, LY294002 had no effect on escape latency in APP/PS1 mice. After DBS, LY294002 partially counteracted the improvement effect of DBS as represented by escape latency ($p < 0.05$). However, LY294002 had no significant impact on swimming speed of mice. In the exploration task, the use of LY294002 did not affect the number of passes and time of occupancy in the target quadrant and platform area. After DBS, LY294002 attenuated but did not counteract the improvement effect of DBS as represented by the number of passes and time of occupancy in the target quadrant and platform area ($p < 0.05$). ELISA showed that soluble Aβ40 and Aβ42 levels were not affected by LY294002 alone in APP/PS1 mice. After DBS, LY294002 partially counteracted the improvement effect of DBS as represented by Aβ40 and Aβ42 levels ($p < 0.05$) (Fig. 11).

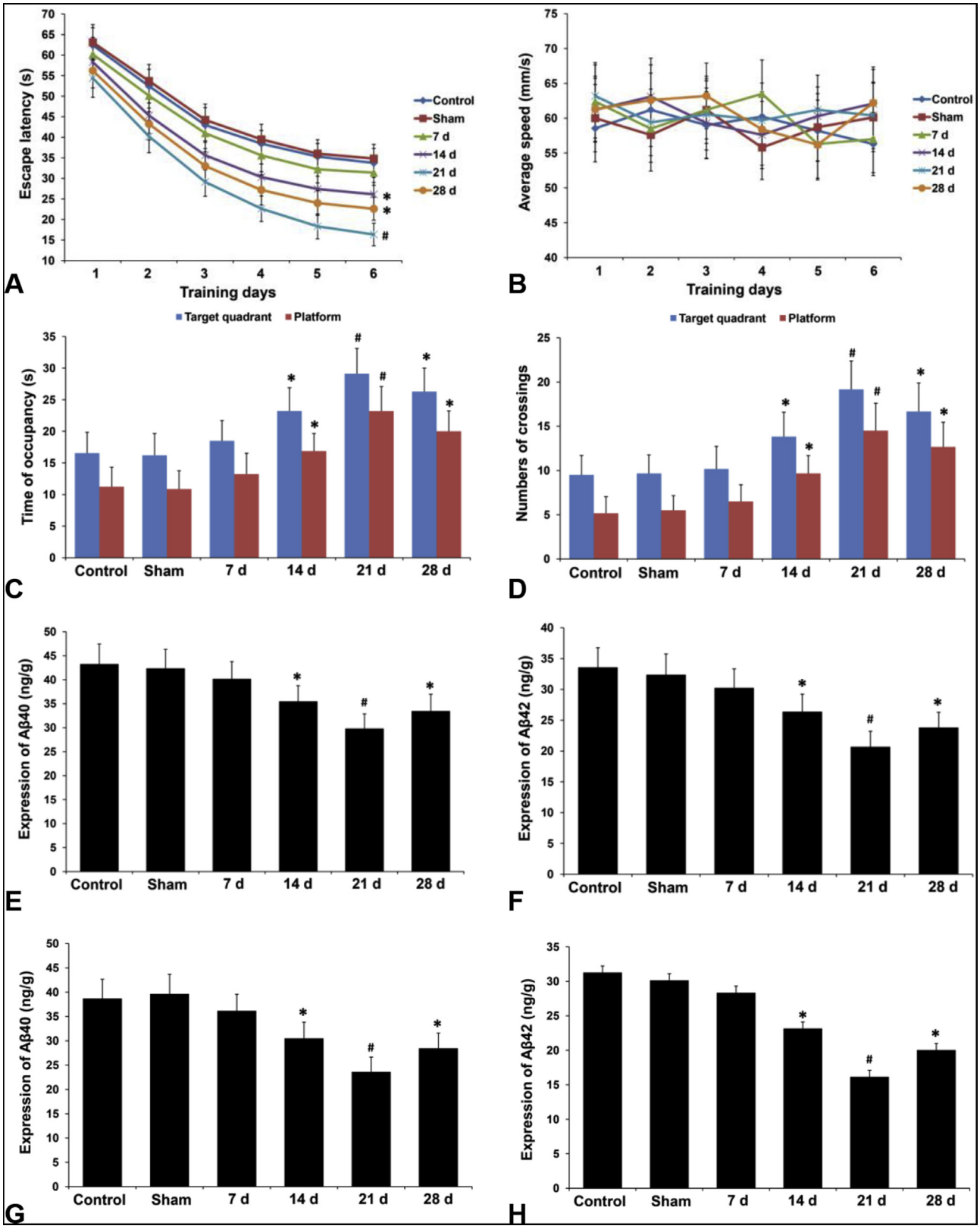

Fig. 4. The effects of different stimulation durations in MWM test and Aβ levels of APP/PS1 mice. (A) Stimulation for 14 days, 21 days and 28 days reduced the escape latency and stimulation for 21 days showed the maximal effect. $^{*}p < 0.05$, vs. sham stimulation group from the second training day; $\#p < 0.05$, vs. other groups from the second training day. (B) Training durations had no impact on the swimming speed. (C, D) Stimulation for 14 days and 28 days increased the number of passes over the target quadrant and platform area (C) as well as the time of occupancy in the target quadrant and platform area (D) significantly, while stimulation for 21 days elicited a further increase. (E–H) DBS for 14 days, 21 days and 28 days could all reduce the soluble Aβ40 (E, G) and Aβ42 (F, H) levels in hippocampus (E, F) and cortex (G, H), and DBS for 21 days caused the greatest reduction of the two soluble protein levels. (C–H) $^{*}p < 0.05$, vs. sham stimulation group; $\#p < 0.05$, vs. other groups.

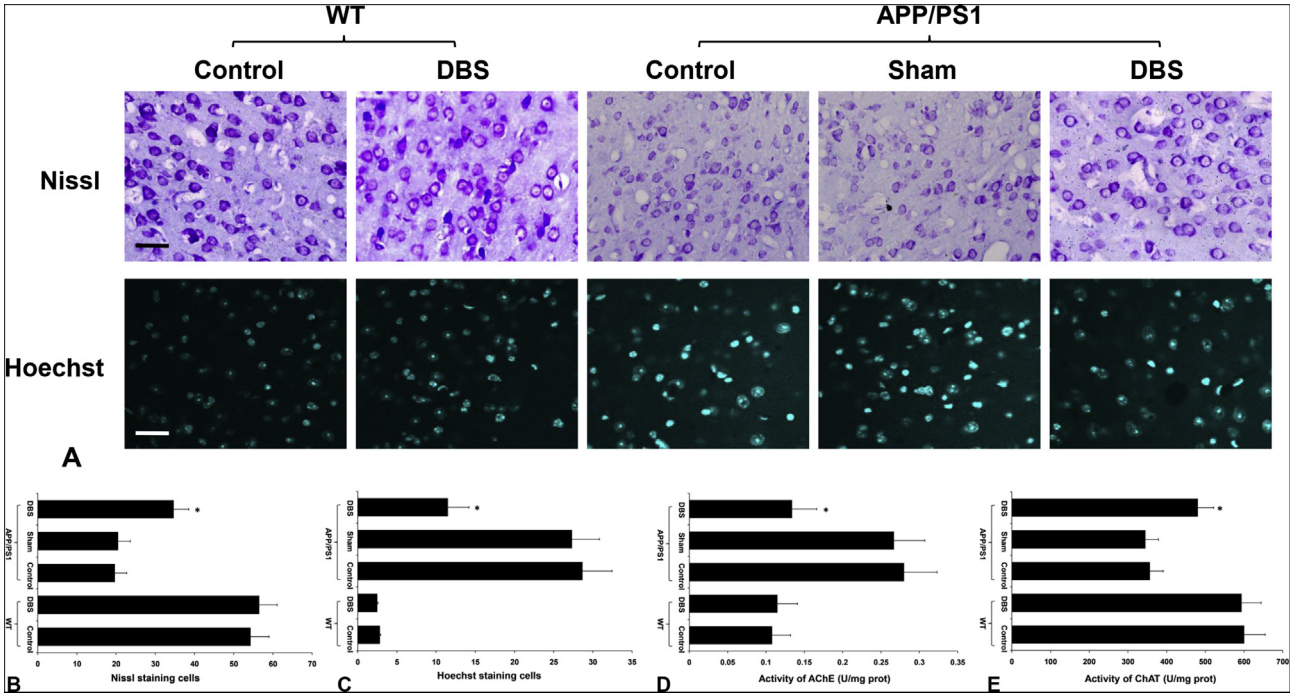

Fig. 5. The effects of DBS in the cortex of each group. The changing trend of the Nissl and Hoechst staining cells was shown in microscopic images. Scale bar: 50 μm (A). DBS had no effect in WT mice. However, DBS increased the number of Nissl positive neurons (B) while decreased Hoechst positive cells (C) in the cortex of APP/PS1 mice. DBS reduced AChE activity (D) while increased the ChAT activity (E) in APP/PS1 mice. $^{*}p < 0.05$, vs. sham.

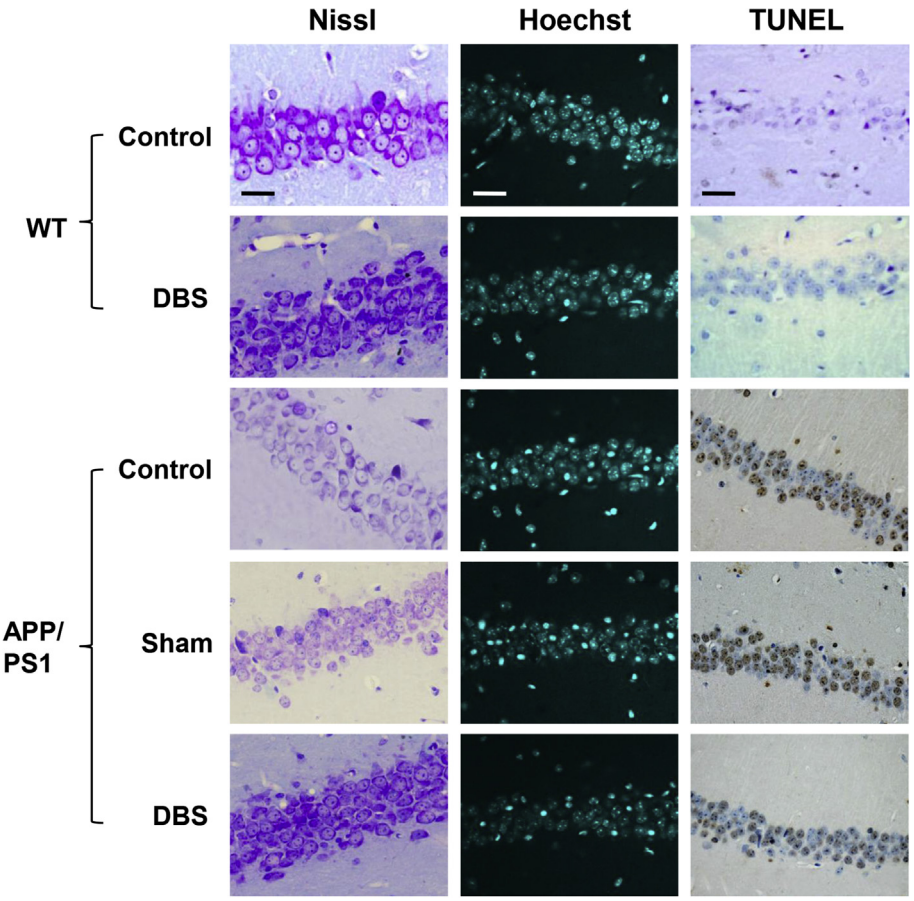

Fig. 6. The effects of DBS on Nissl, Hoechst and TUNEL staining in the hippocampus CA1 region of each group. Scale bar: 50 μm.

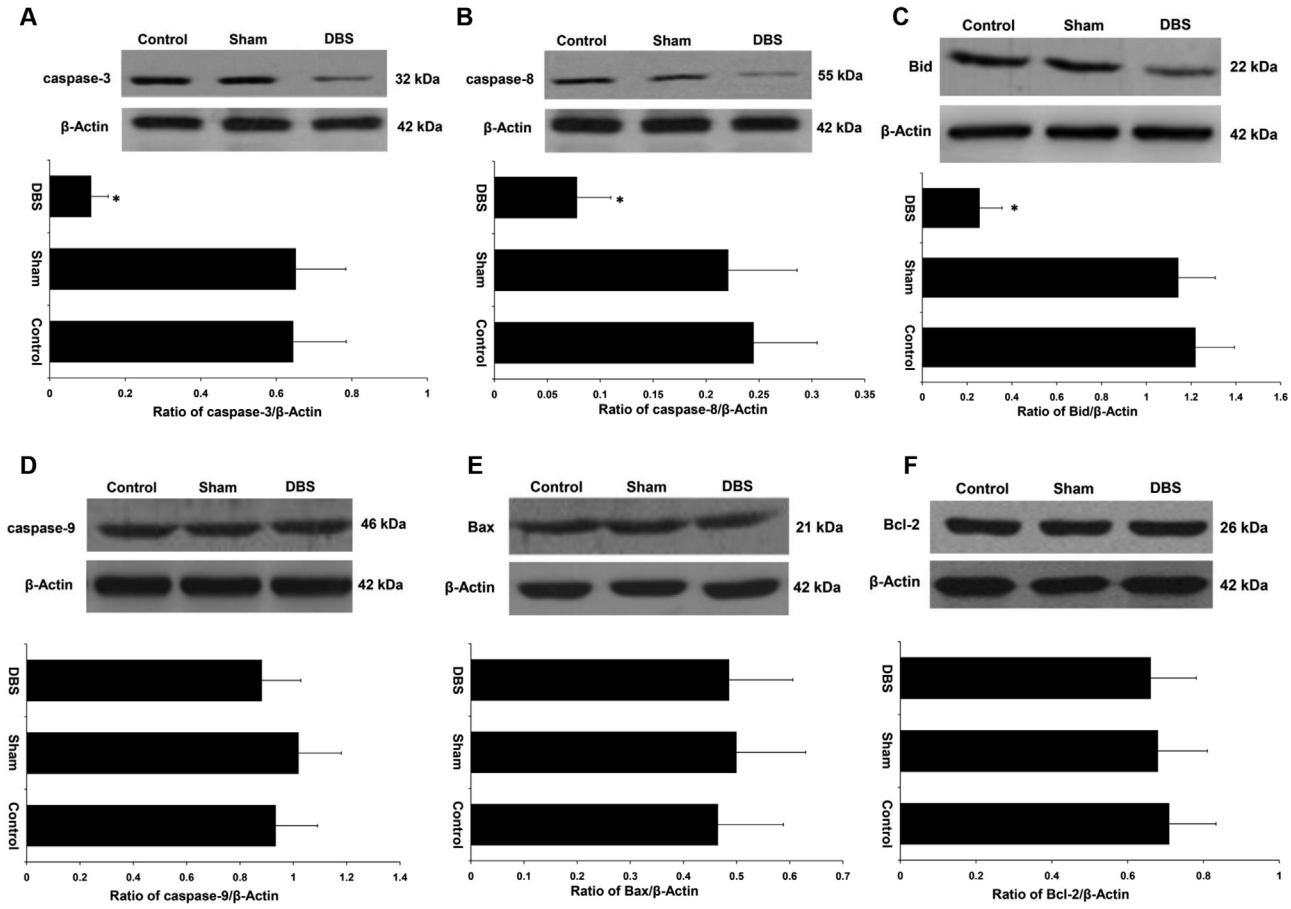

Fig. 7. The effect of DBS on apoptosis related proteins. DBS significantly down-regulated caspase-3 (A), caspase-8 (B) and Bid (C) proteins in APP/PS1 mice, while had no impact on caspase-9 (D), Bax (E) and Bcl-2 (F). $^{*}p < 0.05$, vs. sham stimulation group.

4. Discussion

DBS is now used to treat a variety of diseases, but the choice of target sites and stimulation parameters remains a topic of much discussion. Few studies are devoted to the behavioral effect of long-term DBS on NBM in APP/PS1 mouse models of AD. The present paper assessed the effects of stimulation frequencies, starting time and durations of DBS on NBM in APP/PS1 mouse models of AD by using MWM.

Proper choice of target sites is very important for DBS and the main two targets for AD treatment are possibly fornix and NBM. Several studies have been performed to explore the roles of DBS in the treatment of AD patients, including some randomized, double-blinded trials. Although fornix-DBS displayed positive results, unfortunately, in a recent phase II study, only patients≥65 years rather than all participants benefited [6,7]. It suggests fornix-DBS may be not suitable for the treatment of AD in early stage. Therefore, NBM, as a cluster of nerve cells located between the internal capsule and the ventral pallidum, is possibly an adequate alternative. A few case studies have explored the treatment of cognitive impairment using NBM-DBS. Freund et al. performed bilateral NBM-DBS for one male patient with late-stage Parkinson's disease dementia, who achieved amelioration of dementia [10]. Barnikol et al. proved that NBM-DBS could greatly improve the cognitive functions including memory [18]. However, differential treatment effects of NBM-DBS may be related to the difference in the type of cognitive impairment, course of disease, stimulation parameters or unilateral or bilateral DBS. The clinical trials of NBM-DBS for dementia are now underway, and it is indicated that NBM-DBS can improve AD-associated symptoms with increased cerebral glucose metabolism [11]. Although cholinergic neurons originating from NBM mainly project to neocortex, there are also projections directed to the hippocampal regions [8]. Meanwhile, hippocampus is significant for learning and memory, and is also the main pathological target of Alzheimer's disease. Therefore, to explore the mechanisms of NBM-DBS in AD treatment, we mainly investigated the changes in the hippocampus. Moreover, previous studies have demonstrated functions of hippocampus were influenced by NBM lesions [19]. Our results from cortex and hippocampus were consistent with each other. Although previous sporadic human studies applied bilateral NBM-DBS, our preliminary experiment demonstrated that bilateral NBM-DBS caused more severe complications and higher mortality. In contrast, unilateral stimulation also displayed favorable neuroprotective effects with reversible side effects. Moreover, as pedunculopontine nucleus-DBS for gait freezing in patients with Parkinson's disease, either unilateral or bilateral DBS seems to improve the symptom [20]. As a result, considering the unique anatomy and functions of NBM, unilateral DBS at NBM was performed in APP/PS1 mouse models of AD.

MWM is a behavioral test for hippocampus-dependent spatial learning and long-term spatial memory in rodents. It has a number of advantages, such as simple and fast execution, possibility of differentiating spatial learning from long-term spatial memory, testing of non-spatial abilities, reduction of olfactory interferences and low costs [21]. Meanwhile, previous studies have successfully used MWM to test spatial memory impairment in models of AD

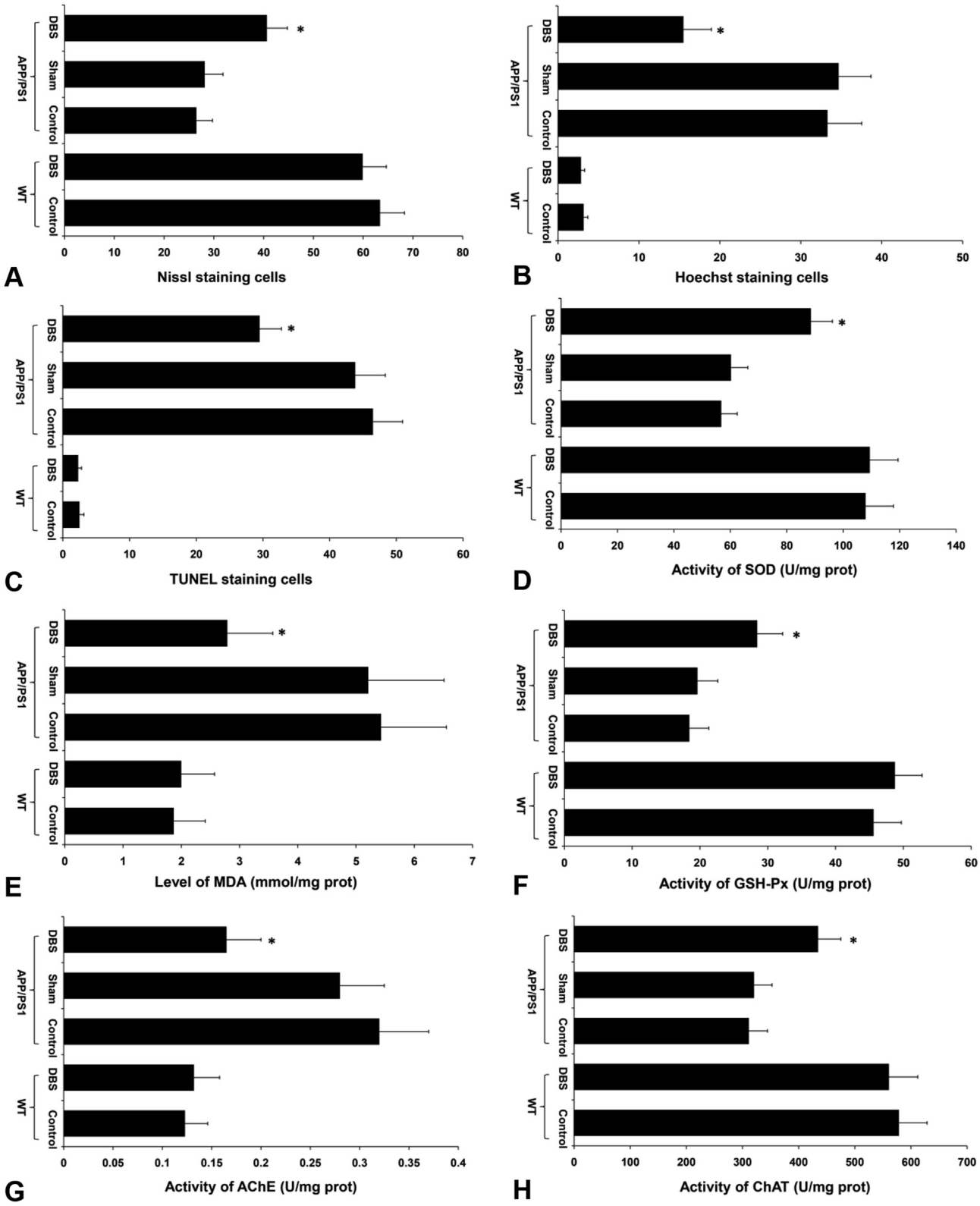

Fig. 8. The effect of DBS on cell counting, oxidative stress and cholinergic system in the hippocampus of each group. DBS had no influence in WT mice. However, in APP/PS1 mice, DBS increased Nissl positive cells (A), SOD activity (D), GSH-Px activity (F) and ChAT activity (H), while reduced Hoechst staining cells (B), TUNEL staining cells (C), MDA levels (E) and AChE activity (G). $^{*}p < 0.05$, vs. sham group.

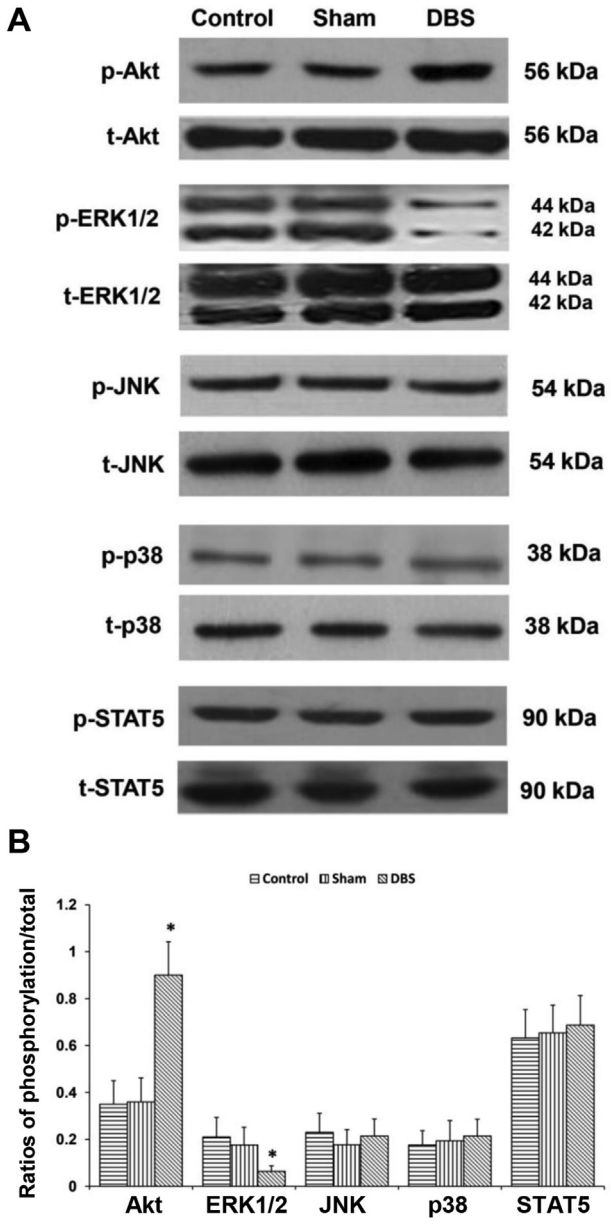

Fig. 9. The effect of DBS on signaling pathway proteins in APP/PS1 mice. DBS up-regulated *p*-Akt/t-Akt while down-regulated *p*-ERK1/2/t-ERK1/2. No impact on *p*-JNK/t-JNK, p-p38/t-p38 or p-STAT5/t-STAT5 expression was observed. (A) Western Blot; (B) Semi-quantitative analysis; $^{*}p < 0.05$, vs. sham stimulation group.

[22,23]. Therefore, MWM was selected as the behavioral tool test to assess the effects of DBS. DBS was performed at 4 frequencies in APP/PS1 mice, which were 10 Hz, 50 Hz, 100 Hz and 130 Hz. In the MWM test, no significant difference was found in the swimming speed of mice when locating the goal quadrant. Therefore, the effect of impaired vision and movement ability of the four limbs on the performance was excluded in the platform-relocating task. Stimulation at higher frequencies (100 Hz, 130 Hz) outstripped that at lower frequencies (10 Hz, 50 Hz) in nearly all indicators, including escape latencies, number of passes over the platform area and time spent in the goal quadrant. Moreover, stimulation at the frequency of 100 Hz achieved better effects than other frequencies. As we all know, the stimulation frequency is very crucial for therapeutic effects of DBS. In patients with Parkinson's disease, high frequency stimulation is of benefit to movement disorders such as dystonia, while more clinical evidence has shown that some axial motor symptoms may improve with low frequency stimulation [24]. Although low frequency simulation is selected for NBM-DBS to treat AD patients, it is concluded from sporadic reports with very small sample size [11,18]. High frequency simulation is used either for NBM-DBS in animals [25] or fornix-DBS in AD patients [7,26], consistent with our findings. Therefore, the optimal frequency remains unclear. In our work, high frequency (100 Hz) was chosen for DBS through comparing with difference frequencies, which solves the issue of absent frequencies comparison in clinical studies. Therefore, the results may be beneficial to further clinical application.

As indicated by both place navigation and exploration tasks, DBS could better improve the cognitive functions of APP/PS1 mice at a younger age. It was reported that in APP/PS1 double transgenic mice, intraneuronal Aβ40 and Aβ42 staining preceded plaque deposition, which started at 3 months of age [27]. Meanwhile, the Aβ42/Aβ40 ratio was elevated in APP/PS1 mice at 2–3 months of age [28]. Moreover, cognitive deficits are also displayed by MWM test as compared with wild-type mice [29,30]. Therefore, it can be regarded that APP/PS1 mouse at 4 months of age is equal to early stage of AD in human. In addition, in one study, NBM-DBS increased the blood flow of ipsilateral cortex in normal mice aged 4–6 months by over 50% compared to only 25% in mice aged 29–31 months. Besides, for young mice, the expression of neural growth factor (NGF) in the parietal cortex was up-regulated, in contrast to no obvious changes in old-age mice [31]. Accordingly, our results revealed significant difference in MWM test between mice aged 4 months and other age groups. Given that Aβ accumulation already takes place at this age and young mice are more tolerable to the stimulation, the age of 4 months was selected for subsequent experiments. Besides, a clinic research also demonstrated that NBM-DBS offered at an earlier stage of the disease and at younger age may have a favorable impact on disease progression and cognitive functions, in parallel with our results [32].

For cognitive disorders, DBS was conducted for four different durations in the mice and the best effect was achieved by DBS for 21 days. As verified, DBS was conducted under the optimized parameters determined by the preliminary experiments to observe the effect on two Aβ proteins, namely, Aβ40 and Aβ42, which exist in either soluble or insoluble forms. Since the soluble forms were more sensitive to neurological function impairment [33], soluble Aβ proteins were detected. Results showed that under the optimized parameters, DBS caused a down-regulation of soluble Aβ40 and Aβ42 in both hippocampus and cortex. In our work, the involved mechanism was not directly investigated. It was demonstrated that DBS activated PI3K/Akt pathway and inhibited ERK1/2 pathway (for details, see below), which contributes to decreased Aβ levels indicated by the previous studies [34,35]. Meanwhile, DBS up-regulates NGF expression [31], which results in reduced generation of Aβ [36]. The facts above may be the mechanisms of Aβ down-regulation by DBS. Therefore, DBS was further conducted on the mice aged 4 months at 100 Hz for 21 days.

Hippocampal neurons were stained by Nissl staining. It was found that DBS greatly increased the survival rate of hippocampal and cortical neurons in APP/PS1 mice. It was reported that DBS increased the survival of dopaminergic neurons in substantia nigra pars compacta (SNc), indicating the neuroprotective effect of DBS [37,38]. As an important pathophysiological mechanism in AD, cell apoptosis facilitates the progression of AD [39]. To assess cell apoptosis in the hippocampus and cortex of APP/PS1 mice, the cells were stained with TUNEL and Hoechst dye, which found a reduction in apoptotic hippocampal and cortical neurons after DBS. Moreover, according to Western blot, NBM-DBS caused a down-regulation of caspase-3, caspase-8 and Bid, but no significant

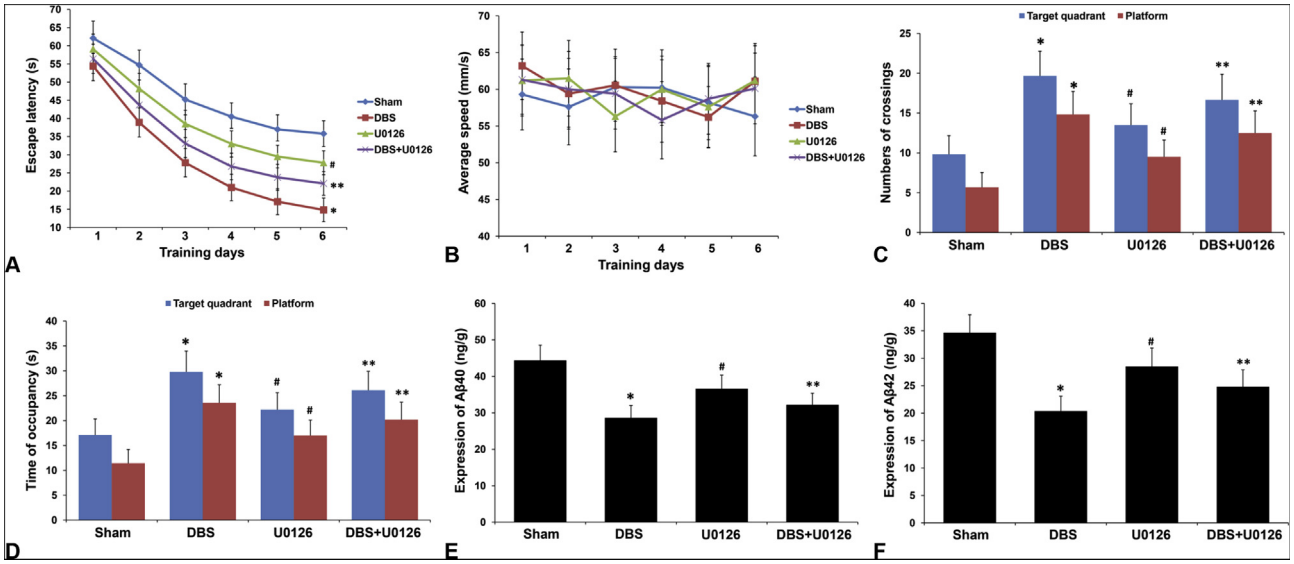

Fig. 10. The effect of U0126 on DBS treatment in APP/PS1 mice. (A) U0126 reduced the escape latency of APP/PS1 mice. After DBS, U0126 partially counteracted the improvement effect of DBS, while the latency was still shorter than that after the use of U0126 but no DBS. #P < 0.05, vs. sham stimulation group from the second training day; $^{*}p < 0.05$, vs. other groups from the second training day; $^{**}p < 0.05$, vs. U0126 and DBS + U0126 from the second training day. (B) U0126 had no impact on the swimming speed. (C, D) U0126 increased the number of passes over the target quadrant and platform area (C) and the time of occupancy in the target quadrant and platform area (D). After DBS, U0126 attenuated but did not counteract the improvement effect. (E, F) ELISA results showed that soluble Aβ40 and Aβ42 levels were reduced by U0126. After DBS, U0126 partially counteracted the effect of DBS on Aβ40 (E) and (F) Aβ42 levels. However, Aβ40 and Aβ42 levels were still lower than those with the use of U0126 but no DBS. (C–F) #$p < 0.05$, vs. sham stimulation group; $^{*}p < 0.05$, vs. other groups; $^{**}p < 0.05$, vs. U0126 and DBS + U0126.

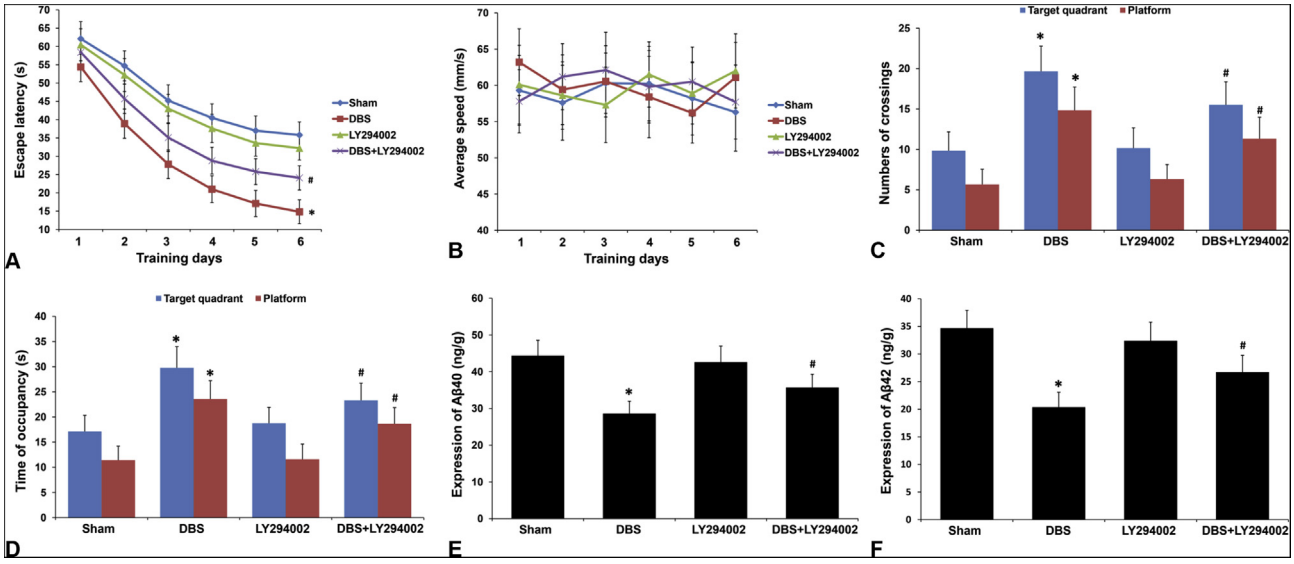

Fig. 11. The effect of LY294002 on DBS treatment in APP/PS1 mice. (A) LY294002 partially counteracted the effect of DBS on escape latency. #$p < 0.05$, vs. sham stimulation group from the second training day; $^{*}p < 0.05$, vs. other groups from the second training day. (B) LY294002 had no significant impact on swimming speed of mice. (C, D) After DBS, LY294002 attenuated but did not counteract the improvement effect of DBS as represented by the number of passes over the target quadrant and platform area (C) and the time of occupancy in the target quadrant and platform area (D). (E, F) LY294002 partially counteracted the down-regulatory effect of DBS on Aβ40 (E) and Aβ42 (F) levels. (C–F) #$p < 0.05$, vs. sham stimulation group; $^{*}p < 0.05$, vs. other groups.

change was found in the expression of caspase-9, Bax and Bcl-2. This suggests that the anti-apoptotic effect of DBS may be related to the exogenous apoptotic pathway, which indirectly triggers the endogenous apoptotic pathway. Although no researches have been published on the role of DBS in cell apoptosis in the AD model, similar effects were reported when DBS was applied to other pathophysiological conditions. Japanese scholars administered NBM-DBS to rats with brain ischemia, and it was found that NBM-DBS reduced delayed neuronal apoptosis in the hippocampus and cortex caused by ischemia [40]. Others pointed out that DBS increased the expression of Bcl-2 and decreased the expression of Bax and caspase-3, thus greatly reducing the cell apoptosis in the hippocampus of animal models of epilepsy [41]. It is generally believed that DBS improves the brain functions and reduces cell apoptosis by up-regulating the anti-apoptotic genes and down-regulating the pro-apoptotic genes [42]. Considering the projecting fibers originating from NBM can be found in hippocampus [8], we speculate that an activation of ACh receptors in the

hippocampus by endogenously released ACh from cholinergic fibers originating from NBM and projecting to hippocampus may contribute to the anti-apoptotic effects of NBM-DBS in hippocampus.

Oxidative stress is another important pathophysiology of AD [43]. Detection of oxidative stress-related factors in the brain showed that DBS reduced the MDA level in the hippocampus and cortex of APP/PS1 mice while increased the activity of SOD and GSH-Px, indicating the protective effect of DBS against oxidative stress. There are a few studies dealing with the correlation between DBS and oxidative stress. For example, Wang et al. found a significant increase in SOD in the cerebrospinal fluid of PD patients after DBS, which was indicative of the anti-oxidative effect of DBS [44], consistent with our results. ChAT is the enzyme related to ACh synthesis while AChE is related to ACh degradation. These two proteins were detected after DBS. The results showed that DBS decreased the activity of AChE in the hippocampus and cortex of APP/PS1 mice while increased the activity of ChAT, indicating that ACh content was increased. NBM-DBS is also regulatory of the cholinergic system. Many studies seem to reveal that NBM-DBS can continuously activate the cholinergic neurons of the basal forebrain area (BFA), leading to local vasodilation and increasing the blood flow to the memory-related cortical region by virtue of the BFA axons projecting into the cortical blood vessels [45]. Moreover, NBM-DBS can promote sensory conduction of the cortex and multisensory integration by altering the excitability of cholinergic neurons and enhancing cortical plasticity [46]. Meanwhile, as reported previously, ChAT activity is decreased while activity of AChE is increased in AD models [47]. Also, DBS seems to induce decreased AChE activity [48]. Moreover, our results suggested that DBS could activate PI3K/Akt pathway (details are below), which contributes to increased ChAT activity and decreased AChE activity in a cognitive deficits model [49]. As a result, it is not difficult to explain the effects of DBD on the activities of AChE and ChAT in our study.

Several signaling pathways are involved in the pathogenesis of AD, including MAPK pathway (JNK, ERK1/2, p38-MAPK) and PI3K/Akt pathway [50]. The results showed that DBS caused a significant up-regulation of *p*-Akt/t-Akt and a down-regulation of *p*-ERK1/2/t-ERK1/2 in the hippocampus of APP/PS1 mice. However, the expressions of *p*-JNK/t-JNK, p-p38/t-p38 and p-STAT5/t-STAT5 were not changed considerably. To verify the effect of DBS on the above pathways, pathway inhibitors were applied. The mice were then assessed with MWM test and Aβ proteins were detected. The use of PI3K inhibitor LY294002 alone could not change the cognitive functions and Aβ protein expressions of mice, which was in agreement with previous studies [14,51]. However, this inhibitor partially counteracted the cognitive improvement effect of DBS as represented by the indicators of escape latency, number of passes over the platform area and the time spent in the goal quadrant. It also weakened the DBS-induced down-regulation of Aβ40 and Aβ42. Considering the DBS-induced up-regulation of *p*-Akt/t-Akt, it was inferred that DBS exerted a neuroprotective effect by activating the PI3K/Akt pathway. Meanwhile, as it was reported that NBM-DBS up-regulated NGF which could activate PI3K/Akt pathway [31,52], we speculate that the activation of PI3K/Akt pathway by NBM-DBS may be associated with the increased release of NGF. In addition, other factors may be also involved by triggering this pathway, which can elicit neuroprotective effects in APP/PS1 mice [53,54]. The failure to completely counteract the neuroprotective effect of DBS may be related to other working mechanisms. The cognitive function could be impaired and Aβ proteins were up-regulated with the use of ERK1/2 inhibitor U0126 alone, which was consistent with other researches [13]. The use of U0126 after DBS weakened the cognitive improvement effect of DBS, affecting the indicators of escape latencies, number of passes over the platform area and time spent in the goal quadrant with a decrease in the expressions of Aβ40 and Aβ42. Therefore, U0126 weakened the neuroprotective effects of DBS possibly due to the inability of DBS eliciting such effects via inhibiting ERK1/2 pathway. Previous studies demonstrated that several drugs like astragaloside and geniposide improved the cognitive functions and reduced Aβ accumulation in AD models by inhibiting the ERK1/2 pathway [55,56]. Additionally, U0126 weakened but did not counteract the beneficial effects of astragaloside, in accordance with our results [55]. To conclude, the protective effects of DBS against AD are attributed to activation of the PI3K/Akt pathway and inhibition of the ERK1/2 pathway.

In conclusion, DBS of NBM at 100 Hz for 21 days starting from 4 months of age could activate PI3K/Akt pathway while inhibit ERK1/2 pathway, which was supposed to be the underlying mechanism of improvement effects of DBS in APP/PS1 mice. Specifically, DBS improved the cognitive functions, increased the survival rate of neurons, reduced cell apoptosis, mitigated oxidative stress and regulated ACh. DBS for mouse models of AD is safe and effective, which provides a new solution for AD treatment. Further studies are required to use different behavioral tests to comprehensively evaluate the effects of DBS on AD, including the pathological, biochemical and molecular biological changes. Ultimately, the applicability of DBS to AD patients requires further investigation.

Disclosure statement

The authors declare no conflicts of interest.

Acknowledgements

This research was supported by grants from the National Natural Science Foundation of China (No. 81500998), Science and Technology Commission of Shanghai Municipality of China (No. 16140903200) and Natural Science Foundation of Shandong Province, China (No. ZR2015PH054).

References

[1] Pereira EA, Green AL, Nandi D, Aziz TZ. Deep brain stimulation: indications and evidence. Expet Rev Med Dev 2007;4:591–603.
[2] Laxton AW, Lozano AM. Deep brain stimulation for the treatment of Alzheimer disease and dementias. World Neurosurg 2013;80:S28. e1–8.
[3] Hu R, Eskandar E, Williams Z. Role of deep brain stimulation in modulating memory formation and recall. Neurosurg Focus 2009;27:E3.
[4] Mirzadeh Z, Bari A, Lozano AM. The rationale for deep brain stimulation in Alzheimer's disease. J Neural Transm 2016;123:775–83.
[5] Sankar T, Chakravarty MM, Bescos A, Lara M, Obuchi T, Laxton AW, et al. Deep brain stimulation influences brain structure in Alzheimer's disease. Brain Stimul 2015;8:645–54.
[6] Laxton AW, Tang-Wai DF, McAndrews MP, Zumsteg D, Wennberg R, Keren R, et al. A phase I trial of deep brain stimulation of memory circuits in Alzheimer's disease. Ann Neurol 2010;68:521–34.
[7] Lozano AM, Fosdick L, Chakravarty MM, Leoutsakos JM, Munro C, Oh E, et al. A phase II study of fornix deep brain stimulation in mild Alzheimer's disease. J Alzheimers Dis 2016;54:777–87.
[8] Gratwicke J, Kahan J, Zrinzo L, Hariz M, Limousin P, Foltynie T, et al. The nucleus basalis of Meynert: a new target for deep brain stimulation in dementia? Neurosci Biobehav Rev 2013;37:2676–88.
[9] Hotta H, Uchida S, Kagitani F, Maruyama N. Control of cerebral cortical blood flow by stimulation of basal forebrain cholinergic areas in mice. Physiol Sci 2011;61:201–9.
[10] Freund HJ, Kuhn J, Lenatz D, et al. Cognitive functions in a patient with Parkinson-dementia syndrome undergoing deep brain stimulation. Arch Neurol 2009;66:781–5.
[11] Kuhn J, Hardenacke K, Lenartz D, Gruendler T, Ullsperger M, Bartsch C, et al. Deep brain stimulation of the nucleus basalis of Meynert in Alzheimer's dementia. Mol Psychiatr 2015;20:353–60.
[12] Paxinos G, Franklin KBJ. The mouse brain in stereotaxic coordinates. second ed. New York: Academic Press; 2001.
[13] Ashabi G, Alamdary SZ, Ramin M, Khodagholi F. Reduction of hippocampal apoptosis by intracerebroventricular administration of extracellular signal-regulated protein kinase and/or p38 inhibitors in amyloid beta rat model of

Alzheimer's disease: involvement of nuclear-related factor-2 and nuclear factor-κB. Basic Clin Pharmacol 2013;112:145–55.
[14] Zhang H, Gao Y, Qiao P, Zhao FL, Yan Y. Fenofibrate reduces amyloidogenic processing of APP in APP/PS1 transgenic mice via PPAR-α/PI3K pathway. Int J Dev Neurosci 2014;38:223–31.
[15] Kaufman AC, Salazar SV, Haas LT, Yang J, Kostylev MA, Jeng AT, et al. Fyn inhibition rescues established memory and synapse loss in alzheimer mice. Ann Neurol 2015;77:953–71.
[16] Chu H, Tang Y, Dong Q. Protection of vascular endothelial growth factor to brain edema following intracerebral hemorrhage and its involved mechanisms: effect of aquaporin-4. PLoS One 2013;8, e66051.
[17] Chu H, Tang Y, Dong Q. Protection of granulocyte-colony stimulating factor to hemorrhagic brain injuries and its involved mechanisms: effects of vascular endothelial growth factor and aquaporin-4. Neuroscience 2014;260:59–72.
[18] Barnikol TT, Pawelczyk NB, Barnikol UB, Kuhn J, Lenartz D, Sturm V, et al. Changes in apraxia after deep brain stimulation of the nucleus basalis Meynert in a patient with Parkinson dementia syndrome. Mov Disord 2010;5:1519–20.
[19] Hosseini N, Alaei H, Reisi P, Radahmadi M. The effects of NBM- lesion on synaptic plasticity in rats. Brain Res 2017;1655:122–7.
[20] Huang C, Chu H, Zhang Y, Wang X. Deep brain stimulation to alleviate freezing of gait and cognitive dysfunction in Parkinson's disease: update on current research and future perspectives. Front Neurosci 2018;12:29.
[21] Ye M, Chung HS, An YH, Lim SJ, Choi W, Yu AR, et al. Standardized herbal formula PM012 decreases cognitive impairment and promotes neurogenesis in the 3xTg AD mouse model of Alzheimer's disease. Mol Neurobiol 2016;53:5401–12.
[22] Liao F, Hori Y, Hudry E, Bauer AQ, Jiang H, Mahan TE, et al. Anti-ApoE antibody given after plaque onset decreases Aβ accumulation and improves brain function in a mouse model of Aβ amyloidosis. J Neurosci 2014;34:7281–92.
[23] Rühlmann C, Wölk T, Blümel T, Stahn L, Vollmar B, Kuhla A. Long-term caloric restriction in ApoE-deficient mice results in neuroprotection via Fgf21-induced AMPK/mTOR pathway. Aging (N Y) 2016;8:2777–89.
[24] Baizabal-Carvallo JF, Alonso-Juarez M. Low-frequency deep brain stimulation for movement disorders. Park Relat Disord 2016;31:14–22.
[25] Nagasaka K, Watanabe Y, Takashima I. Topographical projections from the nucleus basalis magnocellularis (Meynert) to the frontal cortex: a voltage-sensitive dye imaging study in rats. Brain Stimul 2017;10:977–80.
[26] Smith GS, Laxton AW, Tang-Wai DF, McAndrews MP, Diaconescu AO, Workman CI, et al. Increased cerebral metabolism after 1 year of deep brain stimulation in Alzheimer disease. Arch Neurol 2012;69:1141–8.
[27] Wirths O, Multhaup G, Czech C, Feldmann N, Blanchard V, Tremp G, et al. Intraneuronal APP/A beta trafficking and plaque formation in beta-amyloid precursor protein and presenilin-1 transgenic mice. Brain Pathol 2002;12:275–86.
[28] Borchelt DR, Thinakaran G, Eckman CB, Lee MK, Davenport F, Ratovitsky T, et al. Familial Alzheimer's disease-linked presenilin 1 variants elevate Abeta1-42/1-40 ratio in vitro and in vivo. Neuron 1996;17:1005–13.
[29] Xiao Q, Shi R, Yang W, Zou Y, Du Y, Zhang M, et al. Time-dependent increase of Chitinase1 in APP/PS1 double transgenic mice. Neurochem Res 2016;41:1604–11.
[30] Liu Y, Xu YF, Zhang L, Huang L, Yu P, Zhu H, et al. Effective expression of Drebrin in hippocampus improves cognitive function and alleviates lesions of Alzheimer's disease in APP (swe)/PS1 (ΔE9) mice. CNS Neurosci Ther 2017;23:590–604.
[31] Hotta H, Kagitani F, Kondo M, Uchida S. Basal forebrain stimulation induces NGF secretion in ipsilateral parietal cortex via nicotinic receptor activation in adult, but not aged rats. Neurosci Res 2009;63:122–8.
[32] Kuhn J, Hardenacke K, Shubina E, Lenartz D, Visser-Vandewalle V, Zilles K, et al. Deep brain stimulation of the nucleus basalis of Meynert in early stage of Alzheimer's dementia. Brain Stimul 2015;8:838–9.
[33] McLean CA, Cherny RA, Fraser FW, Fuller SJ, Smith MJ, Beyreuther K, et al. Soluble pool of Abeta amyloid as a determinant of severity of neurodegeneration in Alzheimer's disease. Ann Neurol 1999;46:860–6.
[34] Zhang B, Wang Y, Li H, Xiong R, Xiong R, Zhao Z, Chu X, et al. Neuroprotective effects of salidroside through PI3K/Akt pathway activation in Alzheimer's disease models. Drug Des Dev Ther 2016;10:1335–43.
[35] Yun HM, Jin P, Park KR, Jeong HS, Kim EC, Jung JK, et al. Thiacremonone potentiates anti-oxidant effects to improve memory dysfunction in an APP/PS1 transgenic mice model. Mol Neurobiol 2016;53:2409–20.
[36] Triaca V, Sposato V, Bolasco G, Ciotti MT, Pelicci P, Bruni AC, et al. NGF controls APP cleavage by downregulating APP phosphorylation at Thr668: relevance for Alzheimer's disease. Aging Cell 2016;15:661–2.
[37] Temel Y, Visser-Vandewalle V, Kaplan S, Kozan R, Daemen MA, Blokland A, et al. Protection of nigral cell death by bilateral subthalamic nucleus stimulation. Brain Res 2006;1120:100–5.
[38] Wallace BA, Ashkan K, Heise CE, Foote KD, Torres N, Mitrofanis J, et al. Survival of midbrain dopaminergic cells after lesion or deep brain stimulation of the subthalamic nucleus in MPTP treated monkeys. Brain 2007;130:129–45.
[39] Crews L, Masliah E. Molecular mechanisms of neurodegeneration in Alzheimer's disease. Hum Mol Genet 2010;19:R12–20.
[40] Hotta H, Uchida S, Kagitani F. Effects of stimulating the nucleus basalis of Meynert on blood flow and delayed neuronal death following transient ischemia in the rat cerebral cortex. Jpn J Physiol 2002;52:383–93.
[41] Chen N, Gao Y, Yan N, Liu C, Zhang JG, Xing WM, et al. High-frequency stimulation of the hippocampus protects against seizure activity and hippocampal neuronal apoptosis induced by kainic acid administration in macaques. Neuroscience 2014;256:370–8.
[42] Meng DW, Liu HG, Yang AC, Zhang K, Zhang JG. Stimulation of anterior thalamic nuclei protects against seizures and neuronal apoptosis in hippocampal CA3 region of kainic acid-induced epileptic rats. Chin Med J (Taipei) 2016;129:960–6.
[43] Butterfield DA. Evidence of oxidative damage in Alzheimer's disease brain: central role for amyloid beta-peptide. Trends Mol Med 2001;7:548–54.
[44] Wang ES, Yao HB, Chen YH, Wang G, Gao WW, Sun YR, et al. Proteomic analysis of the cerebrospinal fluid of Parkinson's disease patients pre- and post-deep brain stimulation. Cell Physiol Biochem 2013;31:625–37.
[45] Sato A, Sato Y. Regulation of regional cerebral blood flow by cholinergic fibers originating in the basal forebrain. Neurosci Res 1992;14:242–74.
[46] Guzowski JF. Insights into immediate-early gene function in hippocampal memory consolidation using antisense oligonucleotide and fluorescent imaging approaches. Hippocampus 2002;12:86–104.
[47] Soodi M, Saeidnia S, Sharifzadeh M, Hajimehdipoor H, Dashti A, Sepand MR, et al. Satureja bachtiarica ameliorate beta-amyloid induced memory impairment, oxidative stress and cholinergic deficit in animal model of Alzheimer's disease. Metab Brain Dis 2016;31:395–404.
[48] Kádár E, Ramoneda M, Aldavert-Vera L, Huguet G, Morgado-Bernal I, Segura-Torres P. Rewarding brain stimulation reverses the disruptive effect of amygdala damage on emotional learning. Behav Brain Res 2014;274:43–52.
[49] Qi Z, Xu Y, Liang Z, Li S, Wang J, Wei Y, et al. Baicalein alters PI3K/Akt/GSK3β signaling pathway in rats with diabetes-associated cognitive deficits. Int J Clin Exp Med 2016;8:1993–2000.
[50] Simpson JE, Ince PG, Shaw PJ. Microarray analysis of the astrocyte transcriptome in the aging brain: relationship to Alzheimer's pathology and APOE genotype. Neurobiol Aging 2011;32:1795–807.
[51] Zhang Y, Yin F, Liu J, Liu Z. Geniposide Attenuates the Phosphorylation of Tau protein in cellular and insulin-deficient APP/PS1transgenic mouse model of Alzheimer's disease. Chem Biol Drug Des 2016;87:409–18.
[52] Kim MS, Shutov LP, Gnanasekaran A, Lin Z, Rysted JE, Ulrich JD, et al. Nerve growth factor (NGF) regulates activity of nuclear factor of activated T-cells (NFAT) in neurons via the phosphatidylinositol 3-kinase (PI3K)-Akt-glycogen synthase kinase 3β (GSK3β) pathway. J Biol Chem 2016;289:31349–60.
[53] Hong Y, An Z. Hesperidin attenuates learning and memory deficits in APP/PS1 mice through activation of Akt/Nrf2 signaling and inhibition of RAGE/NF-κB signaling. Arch Pharm Res 2018;41:655–63.
[54] Dionísio PA, Amaral JD, Ribeiro MF, Lo AC, D'Hooge R, Rodrigues CM. Amyloid-β pathology is attenuated by tauroursodeoxycholic acid treatment in APP/PS1 mice after disease onset. Neurobiol Aging 2015;36:228–40.
[55] Chang CP, Liu YF, Lin HJ, Hsu CC, Cheng BC, Liu WP, et al. Beneficial effect of astragaloside on Alzheimer's disease condition using cultured primary cortical cells under β-amyloid exposure. Mol Neurobiol 2016;53:7329–40.
[56] Lv C, Wang L, Liu X, Yan SS, Wang Y, Zhang W. Multi-faced neuroprotective effects of geniposide depending on the RAGE-mediated signaling in an Alzheimer mouse model. Neuropharmacology 2015;89:175–84.